HHS Public Access

Author manuscript

J Psychopharmacol. Author manuscript; available in PMC 2015 May 11.

Published in final edited form as:

J Psychopharmacol. 2014 November ; 28(11): 1030–1040. doi:10.1177/0269881114550354.

Resting state functional magnetic resonance imaging reveals distinct brain activity in heavy cannabis users – a multi-voxel pattern analysis

H Cheng[1], **PD Skosnik**[2], **BJ Pruce**[1], **MS Brumbaugh**[2], **JM Vollmer**[2], **DJ Fridberg**[1], **BF O'Donnell**[1], **WP Hetrick**[1], and **SD Newman**[1]

[1]Department of Psychological and Brain Sciences, Indiana University, Bloomington, IN, USA

[2]Department of Psychiatry, The Yale University School of Medicine, New Haven, CT, USA

Abstract

Chronic cannabis use can cause cognitive, perceptual and personality alterations, which are believed to be associated with regional brain changes and possible changes in connectivity between functional regions. This study aims to identify the changes from resting state functional magnetic resonance imaging scans. A two-level multi-voxel pattern analysis was proposed to classify male cannabis users from normal controls. The first level analysis works on a voxel basis and identifies clusters for the input of a second level analysis, which works on the functional connectivity between these regions. We found distinct clusters for male cannabis users in the middle frontal gyrus, precentral gyrus, superior frontal gyrus, posterior cingulate cortex, cerebellum and some other regions. Based on the functional connectivity of these clusters, a high overall accuracy rate of 84–88% in classification accuracy was achieved. High correlations were also found between the overall classification accuracy and Barrett Barrett Impulsiveness Scale factor scores of attention and motor. Our result suggests regional differences in the brains of male cannabis users that span from the cerebellum to the prefrontal cortex, which are associated with differences in functional connectivity.

Keywords

Resting state functional magnetic resonance imaging; multi-voxel pattern analysis; cannabis

Introduction

The principal psychoactive constituent in the commonly used drug cannabis, Δ^9-tetrahydrocannabinol (THC) (Gaoni and Mechoulam, 1971), affects the brain via the activation of central cannabinoid-1 receptors (CB1Rs) (Devane et al., 1988; Pertwee et al., 2010). The CB1R is one of the most abundant G-protein coupled receptors in the central nervous system (Egertova and Elphick, 2000; Eggan and Lewis, 2007; Glass et al., 1997;

Corresponding author: H Cheng, Department of Psychological and Brain Sciences, Indiana, University, 1101 E 10th St, Bloomington, IN 47405, USA., hucheng@indiana.edu.

Conflict of interest

The authors declare that there is no conflict of interest.

Herkenham et al., 1990; Pertwee, 1997, 1999; Tsou et al., 1998). Given the widespread distribution of CB1Rs in the mammalian brain, it is of increasing interest to fully understand their mechanism of action.

In the cerebral cortex, the CB1R (through the binding of either endogenous or exogenous cannabinoids), presynaptically inhibits the release of gamma-aminobutyric acid (GABA) (Ali and Todorova, 2010; Bacci et al., 2004; Bodor et al., 2005; Eggan et al., 2007, 2010; Foldy et al., 2006; Hill et al., 2007; Katona et al., 2000). It therefore appears that CB1Rs function as molecular "brakes," regulating the timing and release of GABA, and thus the overall balance of excitatory and inhibitory neurotransmission (Abbott and Chance, 2005; Farkas et al., 2010; Haider et al., 2006). Chronic cannabinoid administration, which is known to cause down-regulation of CB1Rs in both animals and humans (Hirvonen et al., 2011; Sim-Selley et al., 2006; Villares, 2007), may induce an imbalance in excitatory versus inhibitory tone, which could account for the cognitive, perceptual and personality alterations observed in chronic cannabis users (Fridberg et al., 2010; Ranganathan and D'Souza, 2006; Sewell et al., 2010).

This neural balance at a systems level in humans could be manifested by structural and task-related functional changes of the brain (Batalla et al., 2013). For example, it has been shown that heavy cannabis use is able to induce changes in brain structures such as the hippocampus, precentral gyrus, fusiform gyrus and cerebellum (Cousijn et al., 2012; Matochik et al., 2005; Yücel et al., 2008), and alter brain functions in various regions such as the medial and dorsal parietal cortex, dorsal lateral prefrontal cortex, parahippocampus, anterior cingulate cortex, insula, cerebellum, middle frontal regions, precuneus, lingual gyrus, precentral gyrus, cingulate gyrus, superior frontal gyrus and inferior frontal gyrus (Bolla et al., 2005; Chang et al., 2006; Hester et al., 2009; Jager et al., 2007; King et al., 2011; Schweinsburg et al., 2008, 2010; Van Hell et al., 2009; Wesley et al., 2011). As a result it may influence affective and cognitive operations. For example, in a go/no-go response inhibition task administered by Hester et al., cannabis users showed a significant deficit in awareness of commission errors. A significant difference in the blood oxygenation level dependent (BOLD) response was observed in the anterior cingulate cortex, right insula, bilateral inferior parietal, and middle frontal regions (Hester et al., 2009).

Most of the functional neuroimaging studies in chronic cannabis users employed an activation task. While a specific task may evoke differential brain activation or functional connectivity strength in cannabis users and controls, as demonstrated by previous studies (Behan et al., 2013; Harding et al., 2012; Schweinsburg et al., 2008, 2010; Van Hell et al., 2009; Wesley et al., 2011), task-related differences can be due to a number of factors including individual differences in cognitive ability and strategy use. An alternative approach is to examine brain function when no specific tasks are involved, or the study of the resting state. A recent study comparing resting functional magnetic resonance imaging (fMRI) data in 36 subjects with several thousand activation maps from 30,000 subjects from the BrainMap database showed that functional networks associated with a particular cognitive task are also highly connected at rest (Smith et al., 2009). Therefore, the use of resting state connectivity in the study of chronic cannabis use should reveal similar affected regions/networks. Furthermore, exploring connectivity at rest may provide further

information regarding the nature of the relationship between chronic cannabis use and differences in the neural system; for example, it is not clear whether specific regions are significantly affected by chronic cannabis use or whether a collection of regions within a network is affected and therefore a better indication of heavy cannabis use.

Recently, resting state fMRI data has drawn increasing interest as a way to identify biomarkers for different brain disorders and diseases (Broyd et al., 2009, Collin et al., 2011, Damoiseaux, 2012, Johnson et al., 2012). Resting fMRI may be particularly useful in the study of drug-abuse and psychiatric populations, as there are no task demands, thus ruling out confounds related to behavioral performance. Only recently has resting fMRI been used to explore the brain differences related to cannabis use. One such study revealed two elements within the fronto-temporal network related to cannabis use: the middle frontal gyrus related to high cannabis use and the middle temporal gyrus related to low cannabis use (Houck et al., 2013). Another resting state fMRI study of adolescent cannabis users found increased fractional amplitude of low-frequency fluctuations in the cannabis-dependent population in various regions including superior parietal gyrus, superior frontal gyrus, inferior frontal gyrus, inferior semilunar lobe of the cerebellum, and the inferior temporal gyrus (Orr et al., 2013). Furthermore, higher correlation scores between bilateral inferior parietal lobules and the left cerebellum was reported for cannabis users in both task and resting state fMRI (Behan et al., 2013).

Most studies of the resting state fMRI signal have been focused on analysis in the temporal domain, or exploring the coherence of brain activity among different brain regions when no specific task is involved. Another way of exploring resting brain function is pattern analysis, which has been used to extract particular spatial patterns as mental representations that can be modulated by cognitive states due to external stimuli or intrinsic disorders. For instance, multi-voxel pattern analysis (MVPA) has been successfully applied in classifying patterns of fMRI activation evoked by various categories of visual objects and classifying subjects with mental diseases from normal controls (Cox and Savoy, 2003, Meier et al., 2012). Because MVPA uses multiple voxels, the sensitivity is higher than single-voxel-based analysis. For example, a recent study applying MVPA in resting state fMRI (rfMRI) data identified a number of regions showing distinctive activity patterns in heroin-dependent individuals from normal controls (Zhang et al., 2011). The method employed non-negative matrix factorization (NMF) to extract the spatial feature of each voxel from the time courses of its neighbors and run voxel-based support vector machine (SVM) on a total number of 25 subjects. Compared to other methods such as principle component analysis or independent component analysis, NMF is believed to produce more meaningful dimension reduction of the data and reduce intrinsic noise and is therefore well suited for processing fMRI data (Anderson et al., 2013; Lohmann et al., 2007). Despite the small sample size, their findings agree with other studies using different approaches.

There are two key steps in MVPA: feature selection and classifier training. Feature selection involves selecting voxels or regions to be included in the analysis and constructing features based on the spatial and temporal information of the voxels, and classifier training uses some models to extract relations between patterns and experimental conditions. MVPA can then be applied on a new pattern to predict which condition that pattern is associated with.

The purpose of the present study was to explore rfMRI network differences in chronic cannabis users. This was done by examining the distinctive brain activity patterns of rfMRI using MVPA in a group of carefully screened, heavy cannabis users and controls. The study utilized rfMRI to focus on BOLD activation during non-goal directed activity. SVM-based MVPA was applied on neighbors of each voxel in the gray matter to identify the regions that were distinctive between cannabis users and normal controls. In order to validate the findings of the MVPA analysis, mean accuracy of all the voxels for each cannabis user subject was used to regress against tetrahydrocannabinol (THC) metrics and some behavior data. In addition, pair-wised correlation of mean time courses of each identified region was computed to characterize the functional connectivity between these regions, which was then used as new features for further MVPA analysis to test the accuracy rate of classifying a single subject into either group.

Methods

Participants

Twenty five adult male volunteers participated in this study (13 controls (CTL group); 12 cannabis users (CB group)). Subjects were recruited using posted announcements in the local community. After providing a complete description of the study to all participants, written and verbal informed consent was obtained. Demographic data are presented in Table 1. The research protocol was approved by the Indiana University–Purdue University Indianapolis Human Subjects Review Committee. Participant data were de-identified to protect confidentiality, and all participants were compensated $10 per hour for their participation. Cannabis users who reported past use of three or more non-cannabis illicit substances, reported use of an illicit substance other than cannabis within three months prior to their study participation, or who met criteria for a non- cannabis-related *Diagnostic and Statistical Manual of Mental Disorders, 4th Edition* (DSM-IV) psychopathology were excluded from the study to minimize the influence of those variables on the results. As in previous studies, participants were excluded if they reported the consumption of more than 14 alcoholic drinks (196 g of alcohol) per week during the past month, or more than five drinks (70 g of alcohol) in one single occasion (Fridberg et al., 2010; Skosnik et al., 2006, 2008).

Formal inclusion criteria were the following: (a) for the CB group: current cannabis consumption at the rate of at least once per week during the past month, no other illicit substance use during the past three months, and no DSM-IV diagnosis of Axis I or II disorders except cannabis abuse or dependence; (b) for the CTL group: no history of illicit substance use and no history of psychiatric illness (Axis I or II); (c) for all participants: age 18 years or older, completion of high school education, and no history of cardiovascular disease, disorders of hearing, neurological disease, learning disability, or head injury resulting in loss of consciousness. Subjects in the cannabis group were required to abstain from cannabis use for at least 12 h prior to their participation in the study to eliminate possible acute cannabis effects during imaging. The American National Adult Reading Test (ANART) was used as a measure of pre-morbid intellectual ability. This is based in part on the premise that pronunciation of irregular words is unaffected in many clinical disorders,

and that performance is highly correlated with general intellectual ability (Grober and Sliwinski, 1991, O'Carroll et al., 1992). The Perceptual Aberration Scale (PAS) (Chapman et al., 1978) and Schizotypal Personality Questionnaire (SPQ) (Raine, 1991) were used to assess schizotypal personality characteristics. The Barratt Impulsiveness Scale (BIS), a widely used self-report assessment of impulsivity (Patton et al., 1995, Stanford et al., 2009), yielded measures of attentional, motor, and nonplanning impulsiveness.

The Structured Clinical Interview for DSM-IV Axis I Disorders (SCID-I; First et al., 2002) and a locally developed drug-use questionnaire based on a timeline follow-back approach were used to ascertain current and past diagnoses for substance abuse and dependence, as well as current and past cannabis consumption patterns. Measures of frequency, quantity, and density of cannabis consumption were determined via the SCID-I and questionnaire for the past three months, past month, and past week prior to the test session as described previously (Fridberg et al., 2010; Skosnik et al., 2006, 2008, 2012). Age of first use and total years of use were also determined. Urine screens (Q10-1, Proxam) were administered immediately preceding scanning in order to corroborate self-reports from the drug questionnaire and clinical interview. The Q10-1 kit screens for cannabis (THC-COOH; 50 ng/mL sensitivity), opiates, amphetamines, cocaine, ecstasy (MDMA), tricyclic antidepressants, phencyclidine, benzodiazepines, methamphetamines, and barbiturates. A portion of the urine was aliquoted and stored in opaque tubes at −80°C for later quantitative determination of levels of THC, THC-COOH, and OH-THC.

Urinalysis

THC-COOH—The samples were analyzed by gas chromatography-mass spectrometry (GC-MS). The method employs a basic hydrolysis step that frees THC-COOH (but not THC) from its glucuronide conjugate. Samples were run using a 0.10 mL aliquot size. Duplicate calibrators (1.0 mL with both THC-COOH and THC) were at 0.1, 0.5, 1.0, 2.5, 5, 10, 25, 50 and 100 ng/mL. Due to sample dilution, the THC-COOH calibration curve ranged from 5–1000 ng/mL. Duplicate 1.0 mL (with both THC-COOH and THC) quality control samples (QCs) were included at 1.5, 5 and 80 ng/mL. Triplicate 0.1 mL dilution QCs were included at 150 ng/mL.

THC and OH-THC—Samples were analyzed by GC-MS. Aliquots (1.0 mL) were pretreated with β-glucuronidase for 18 h at 37°C. Samples were then extracted along with the calibrators (0.5–100 ng/mL) and QCs used in the THC-COOH batch described above.

Creatinine—Creatinine was determined using a microplate colorimetric test based on the Jaffe reaction where picric acid reacts with creatinine to form a colored product. Samples were diluted 20-fold (0.025 mL plus 0.475 mL water). Duplicate 0.5 mL calibrators were run at 2, 4, 6, 8, 10, 12 and 15 mg/dL. Due to sample dilution, the calibration range was 40–300 mg/dL. Triplicate diluted QCs were included at 25 and 100 mg/dL. Samples outside the calibration range were repeated using a smaller or larger dilution as needed. THC and THC-COOH concentrations were normalized by creatinine levels to account for differing levels of urine dilution across subjects (THC/Cr and THC-COOH/Cr, respectively).

Imaging data acquisition and analysis

Data acquisition—During the resting state scans participants were instructed to lie with their eyes open and relax, but not to fall asleep. All magnetic resonance imaging (MRI) scans were acquired using a Siemens Tim Trio 3.0-T scanner (Erlangen, Germany) with 32-channel head coil. Subject head motion was minimized with restraining foam pads provided by the manufacturer. Gradient-recalled echo planar imaging (EPI) was used to capture 175 volumes. Interleaved acquisition of 35 axial 3.8 mm slices covering the whole brain were captured using 2500 ms repetition time (TR), 30 ms echo time (TE), 220 mm field of view (FOV), 70° flip angle, and a 128×128 image matrix resulting an in-plane resolution of 1.72 mm. High-resolution T1-weighted MRI volumes were acquired sagittally using the 3D MP-RAGE sequence with the following parameters: 256×256 image matrix with 160 slices, 1×1×1 mm^3 voxels, TE=2.67 ms, TR=1800 ms.

Preprocessing—The resting state EPI volumes were motion corrected in FSL (http://fsl.fmrib.ox.ac.uk/fsl), with all image aligned with the 100^{th} image volume. Relative/absolute translational and rotational motion was extracted from the motion correction output (Van Dijk et al., 2012). All images were normalized to the standardized Montreal Neurological Institute (MNI) T1 template, during which co-registration of each subject's high-resolution T1 weighted image to their mean functional EPI was used for improved accuracy. Segmentation was performed on the MNI 2 mm resolution image using FSL segmentation tool FAST to obtain a probabilistic gray matter image with intensity between 0–1. We used 0.01 as the threshold to set a gray matter mask for subsequent pattern extraction. A voxel-wised searchlight with 6 mm radius was applied on the normalized images within the gray matter (Kriegeskorte et al., 2006). According to Kriegeskorte et al., a searchlight of 4–5 mm radius is optimal or near-optimal. Because the analysis was restricted to gray matter, we relaxed the radius to 6 mm, and found that the number of voxels ranged from 2–123, and the average number of voxels within gray matter was 90, close to the value of 81 that corresponds to a searchlight of 5 mm without gray matter masking. A searchlight radius of 5 mm resulted in an average of 61 voxels within gray matter. For each voxel, a 2D spatial temporal pattern was obtained and represented by an $m \times n$ matrix, with m the number of voxels in the searchlight sphere and n the number of image volumes. A bandpass filter between 0.01 Hz and 0.1 Hz was applied to the time dimension, followed by non-negative matrix factorization performed in Matlab (Mathworks, Natick, Massachusetts, USA), and the largest component was used as the representative pattern of that voxel.

MVPA—MVPA analysis was performed on two levels using a linear support vector machine classifier. First, SVM analysis was run on a voxel basis, using the spatial pattern of the neighboring voxels to find clusters that differentiate the two groups; because this one is based on the resting state activity of each region we called it local MVPA. Second, MVPA was applied on the functional connectivity between the widespread clusters identified in the local MVPA analysis; we called it connectivity-based MVPA. For local MVPA, the feature space was chosen to be the 1D representative pattern containing intensities of m voxels. We used the -Matlab tools from LIBSVM (http://www.csie.ntu.edu.tw/~cjlin/libsvm/). Because coil sensitivity can be different for each scan and each subject due to different head position and brain size, the signal intensity varies between subjects. To reduce the effect of signal

intensity, the voxel-wised pattern was rescaled between 0–1 for each subject. Then for each voxel, we labeled the normal controls as 1 and the cannabis users as −1. The regularization coefficient was chosen to be 1. We adopted the leave-one-out scheme to evaluate the accuracy rate of classifying the subject to a corresponding group on each voxel. Each time, one subject (either control or cannabis user) was set apart, the remaining data was treated as training data. After SVM was run on the training data set, we classified the left-out subject based on the training. If the classification agrees with the true value, the accuracy rate was set to 1; if not, the accuracy rate was 0. This process was applied to each subject, resulting in a total of 25 accuracy values with either 0 or 1. Then we assigned each voxel the average accuracy rate to obtain an image of correct prediction. We further applied an accuracy threshold of greater than 0.70 and the cluster size threshold of greater than 81 voxels (number of voxels corresponding to searchlight radius of 5 mm). Then we obtained a map with regions differentiating normal controls and cannabis users. We pick 0.70 as the threshold for two reasons: first, it is reasonably high; second, the resultant clusters are not too few. This is consistent with previous applications of the method (Zhang et al., 2011).

The pipeline of the data processing for local MVPA is illustrated in Figure 1. After obtaining the map of distinct clusters with accuracy rate higher than 70%, connectivity-based MVPA was performed by using the functional connectivity between the distinct regions as new features. The purpose was to determine whether the distinct regions from local MVPA can be used as a biomarker to distinguish the two groups. First, the mean time course within each cluster was computed for the 25 subjects from the normalized unsmoothed data. Quadratic detrending was then applied on the mean time course, followed by regression of whole brain mean signal of white matter and mean signal of cerebrospinal fluid. The resultant signal was band-pass filtered in the range of 0.01 Hz – 0.1 Hz. The functional connectivity was calculated as cross-correlation of the processed mean time courses. The functional connectivity can be represented by an adjacent matrix with each identified cluster the node and inter-cluster connectivity the edge. The SVM was run on the edge weights (i.e. connectivity strengths) using the leave-one-out scheme. To test the robustness of the method, different thresholds were set from 0–0.25 to remove the weak or negative edges.

Additionally, behavioral measures were correlated with the MVPA results for the cannabis group. This was done to determine whether the overall classification accuracy of the SVM algorithm on cannabis users varies as a function of these measures. Therefore, by averaging the accuracy rate over all the voxels in the thresholded map, a mean accuracy rate was obtained for each subject that to some degree characterizes the probability of that subject being a cannabis user. The correlation between the mean accuracy value and behavior measurements was then examined. There are many behavioral measurements. We only selected those that were significantly different from the control group, which included total SPQ, PAS, BIS-Attention, BIS-Motor. We also investigate the relation between the mean accuracy value and age of onset for cannabis use. To investigate the relation between the accuracy rate and THC usage, a THC classification index (TCI) was assigned to each cannabis user based on their urine THC-COOH/creatine ratio. The index was calculated by fitting the THC-COOH/creatine ratio to the logistic function shown in Equation 1 to obtain a quantity that characterizes the degree to which a subject belongs to the CB group.

$$L=\frac{1}{1+\exp(-\alpha C)} \quad (1)$$

For positive C (THC-COOH/creatine ratio) and parameter α, the output is a number between 0.5–1. We adjusted the parameter α so that the mean value of L from all 12 subjects is equal to the mean accuracy rate. We call the output L of the corresponding logistic function TCI. The correlation between the mean accuracy rate and TCI was then calculated.

Results

Behavioral and cannabinoid metabolite data

Demographic data for both participant groups are shown in Table 1. Nine of the 12 cannabis participants met DSM-IV criteria for cannabis abuse or dependence. In order to examine the veracity of participants self-reported recency of cannabis use, correlation coefficients were calculated examining the relationship between number of joints smoked in the past week and urinary cannabinoid levels. In order to control for urine dilution, metabolite levels were normalized to urinary creatinine levels. Both THC (r=0.721, p<0.008) and its active metabolite OH-THC (r=0.664, p<0.02) correlated significantly with number of joints in the past week, while the inactive THC metabolite THC-COOH (r=0.38, p<0.22) did not, thus providing corroboration of the self-reported cannabis use data. There is no significant difference in the head motion parameters.

Local MVPA analysis

Several regions were identified that distinguish the CB and CTL groups with high confidence in SVM pattern analysis on the resting state fMRI time series. The regions showing difference between the two groups with classification accuracy rate >70% are displayed on a 3D rendered brain in Figure 2. Eleven clusters distributed in the cerebrum and cerebellum were found to distinguish between the cannabis users and normal controls in the SVM analysis (see Table 2). Because there is no smoothing in the preprocessing, the voxels in the clusters are not smooth clusters. The clusters were located in the precentral gyrus, middle frontal gyrus, cingulate gyrus, superior frontal gyrus, posterior cingulate, inferior frontal gyrus, inferior temporal gyrus/fusiform gyrus, and cerebellum. The corresponding locations in 2D axial slices are shown in Figure 3. From Table 2, the volume of the region was in the order of 100 mm^3. The mean accuracy rate is very close for each region, ranging from 75.2–77.4%. No bilateral symmetry of the regions was observed except for the middle frontal gyrus.

The scatter plots depicting the correlation between some behavior measures and mean accuracy rate from SVM are shown in Figure 4. The mean accuracy rate was highly correlated with BIS-Motor with a correlation coefficient of 0.76 and p value of 0.004, and was correlated with BIS-Attention with a correlation coefficient of 0.44 and p value of 0.15. A trend of positive relationship between age of onset and mean prediction rate is also exhibited: the correlation coefficient is 0.29 if including all subjects, and the correlation coefficient is 0.44 if excluding a possible outlier, for which age of onset is 11 years. The urine THC-COOH/Creatinine ratio ranged from 0.0343–3.147. The THC classification

indices derived from the THC-COOH/Creatinine ratio was between 0.519–0.999. The correlation coefficient between the two was 0.46 with *p* value=0.13. There was little correlation between mean accuracy rate and total SPQ (r=0.09) or between mean accuracy rate and PAS (r= −0.05).

Connectivity-based MVPA analysis

The mean functional connectivity between the regions for two groups is shown as an adjacent matrix in Figure 5(a) and 5(b). Because we are only interested in the inter-cluster connectivity, the diagonal of the matrix was set to zero. The mean connectivity strength ranged from −0.05 to 0.40. The difference of connectivity shown in Figure 5(c) connectivity indicates that CB group tends to have higher connectivity strength than CTL group. Among all the connectivity, the cingular gyrus showed strongest connectivity with MFG1 and PCG2. The precentral gyrus, middle frontal gyrus, and post cingulate cortex tended to have stronger connectivity with other distinct regions compared to other nodes. It is also noted that the connectivity strength fluctuated substantially from subject to subject, as indicated by the matrix of standard deviation (Figure 5(d)). The standard deviation is comparable to the difference of connectivity strength between the two groups.

Accuracy rate higher than 80% in classifying a subject as a cannabis user or not was obtained when using the connectivity strengths as feature space for SVM analysis. The high accuracy rate is very stable against thresholding. Table 3 lists accuracy rates at different thresholding criteria. The overall accuracy rate was 84% if all the edges in the adjacent matrix were used in SVM, corresponding to a 55 dimensional feature space. The accuracy rate varied between 84–88% as the dimension of the feature space dropped from 55 to 14 at different thresholds. In all conditions, the accuracy of classifying CB group or CTL group was consistently above 83%.

Among all the inter-cluster connectivity, some showed significant difference (p<0.05 from two-sample *t*-test without correction for multiple comparisons) between the CTL group and the CB group. The CB group showed higher connectivity strength in five pairs, (PCG1, MFG2), (PCG1, SFG), (MFG1, CGG), (CGG, SFG), and (IFG, FSG).

Discussion

We have demonstrated that a two-level MPVA can be used to classify cannabis users from normal controls. The first level MVPA works on a voxel basis and identifies regions for the input of a second level MVPA, which works on the functional connectivity between these regions. We found a high overall accuracy rate of 84–88% in predicting whether a single subject is a cannabis user, and this rate is significantly higher than by chance, which is 50%. The high accuracy rate was consistent across different thresholds, making the accuracy rates unlikely to be due to the randomness of the algorithm. The high accuracy rate suggests local changes may occur in the brains of cannabis users that span from the cerebellum to the prefrontal cortex and that local change may also lead to differences in functional connectivity.

The two MVPA methods are complementary. The feature space of local MVPA is extracted from spatiotemporal information of voxel neighbors while in the connectivity-based MVPA, the feature space is the correlation of the time courses of various regions. The advantage of the two-level analysis is that the connectivity-based global level is a confirmation of findings from the local level. All the clusters identified in this study lie in disparate regions across the brain and they all have shown differences between CTL and CB groups in previous structural and functional studies. For example, regions such as the medial and dorsal parietal cortex, dorsal lateral prefrontal cortex, cerebellum, middle frontal regions, precentral gyrus, cingulate gyrus, superior frontal gyrus and inferior frontal gyrus have all been found previously to be associated by cannabis use (Chang et al., 2006; Matochik et al., 2005; Orr et al., 2013; Schweinsburg et al., 2008; Van Hell et al., 2009; Wesley et al., 2011). For instance, the superior frontal gyrus region identified by Orr et al. (2013) using rfMRI procedures is similar to the SFG reported here.

One region in particular coincides with the findings from a structural study of the same subjects using diffusion tensor imaging and network analysis (Kim et al., 2011); the posterior cingulate cortex (PCC) showed altered local network organization. The PCC is considered a key region in the default mode network (DMN) and is thought to sustain a sense of self-consciousness and is engaged in self-referential mental thoughts during rest (Buckner and Carroll, 2007; Cavanna and Trimble, 2006). In addition to the local structural network differences in the PCC, Kim et. al. (2011) also observed global network differences between CTL and CB groups – differences in the normalized clustering coefficient and network efficiency. These differences suggest that cannabis user subjects have differences in the capacity to perform local processing and that the transfer of information across the brain may be less efficient. These structural network differences appear to be analogous to the local changes in multiple regions widely distributed throughout the brain, changes that are shown here examining resting state brain function and connectivity.

Other drug studies using resting state fMRI also revealed similar regions that exhibit differences between drug users and normal controls. In a recent study of adolescent cannabis users, altered resting-state connectivity was found in the superior frontal gyrus, right superior parietal gyrus, and the cerebellum in the cannabis users compared to non-users (Orr et al., 2013). Another study showed greater activity and functional connectivity for high risk adolescent cannabis users than low cannabis users in left middle frontal gyrus (Houck et al., 2013). The greater activity for high cannabis users is in line with our findings of significant higher connectivity strengths for five pairs of clusters. The PCC and insula have also been found to be two critical regions showing differences in the strength of functional connectivity (Pujol et al., 2013). In the study of heroin addiction using SVM, regions found include orbitofrontal cortex, medial frontal cortex, inferior frontal cortex, superior frontal cortex and cingulate gyrus. Also, Wei and colleagues observed decreased functional connectivity in the PCC and the medial prefrontal cortex in a sample of heroin users (Wang et al., 2010). More recently, Chanraud et al. (2011) showed that resting state low frequency fMRI signals in the posterior cingulate and cerebellum were less synchronized in alcoholics than in controls, indicative of decreased functional connectivity. A study of concurrent MDMA and cannabis users also showed smaller task-induced deactivations of the DMN compared to healthy participants (Roberts and Garavan, 2010). It appears that

hypoconnectivity between brain regions of the DMN might be a common characteristic of substance-seeking individuals. While speculative, this decrease in temporal coherence and hypoactivity of the DMN may represent a neural correlate of altered self-referential processing and increased impulsivity (disinhibition), both commonly observed characteristics in substance seeking individuals (De Wit, 2009; Newlin and Renton, 2010).

Our results show higher correlation or functional connectivity strength between several clusters for the CB group. This might be due to a general cannabis-related hyperconnectivity between brain regions as revealed by task fMRI and rfMRI in spite of different regions selected in these studies (Behan et al., 2013; Harding et al., 2012). Another interesting finding here is the correlation between prediction accuracy and behavioral measures. As shown in the scatter plots in Figure 4, a reasonably strong correlation between mean accuracy rate from SVM and BIS-scores of motor impulsivity was found. In other words, individuals with higher BIS-motor scores were better classified using these regions than those with lower scores. THC has been found previously to impact psychomotor functioning (Dumont et al., 2010; Ranganathan and D'Souza, 2006). Also in a study exploring motor processing during a maze task, Weinstein et al. (2008) found that THC resulted in increased activation of areas involved in the coordination and planning of movement. Interestingly, here regions linked to motor processing (the precentral gyrus, and the cerebellum) as well as control, including motor control (the middle frontal and anterior cingulate cortex) were all found to accurately classify cannabis users. The finding that classification accuracy was higher for those with higher scores (the CB group had higher scores, on average, than the CTL group) may suggest that MVPA may be sensitive to these motor differences.

Despite many findings that were consistent in general with previous studies, we did notice some discrepancies. The exact location of the distinct regions was slightly different from those reported earlier (Houck et al., 2013; Orr et al., 2013). For example, the middle frontal gyrus identified in our study is more anterior than that reported by Houck et al.; the inferior temporal lobe is in the opposite hemisphere as reported by Orr et al. The positive correlation between age of onset and mean prediction rate shown in Figure 4(c) was in line with previous findings that age of onset is associated with structural and functional changes (Gruber and Yurgelun-Todd, 2005, Harding et al., 2012), however the effect was not significant. Also the correlation between duration of cannabis use and mean prediction rate failed to reach significance. These differences could be attributed to the analysis method, the small sample size, and large variability of cannabis use.

There are several limitations to the current study. First, the cross-sectional design of the study precludes the ability to ascertain the precise cause and effect relationships. Hence, it remains unclear whether the observed results were due to the residual effects of THC, cannabis withdrawal, long-term cannabis exposure (e.g. CB1R downregulation), or premorbid neurodevelopmental and/or personality differences predisposing individuals to use cannabis. Second, while cannabis use rates where very high for each of the subjects in the cannabis group, 3/12 of the subjects did not meet criteria for cannabis abuse/dependence. Thus, the slight heterogeneity of the group could have affected the between group analysis. Third, there were a relatively small number of subjects, and our analysis of the relationship between the behavior and the accuracy rate of SVM in the distinctive regions was

exploratory in nature. Lastly, there is some freedom in running the SVM algorithm such as varying the regularization parameter. How to optimize the SVM algorithm with different number of features and signal-to-noise ratios needs further investigation. These limitations could be addressed in future rfMRI studies examining the effect of both acute and chronic cannabinoid exposure utilizing a larger sample of human participants.

Lastly, it should be noted that motion is a potential confound that can have an impact on connectivity data. Motion introduces more noise and creates unwanted coherence of the time course. While there are ways to reduce motion effects, examination of motion prior to analysis and setting strict exclusion criteria are extremely important. We were very sensitive to the issue of motion here and ensured that there were no significant differences between groups and kept the movement for any participant included in the analysis low (within 0.6 mm).

Acknowledgments

The authors are grateful to Dr. Yi Zhang for discussion of the methods.

Funding

This research was supported by the National Institute on Drug Abuse (1 R21 DA023097-01A1 to PD Skosnik), and the National Institute of Mental Health (R01 MH62150 and 1 R21 MH091774-01 to BF O'Donnell; R01 MH074983 to WP Hetrick).

References

Abbott LF, Chance FS. Drivers and modulators from push-pull and balanced synaptic input. Prog Brain Res. 2005; 149:147–155. [PubMed: 16226582]

Ali AB, Todorova M. Asynchronous release of GABA via tonic cannabinoid receptor activation at identified interneuron synapses in rat Ca1. Eur J Neurosci. 2010; 31:1196–1207. [PubMed: 20345910]

Anderson A, Douglas P, Kerr W, et al. Non-negative matrix factorization of multimodal MRI, FMRI and phenotypic data reveals differential changes in default mode subnetworks in ADHD. Neuroimage. 2013 EPub ahead of print. 10.1016/j.neuroimage.2013.12.015

Bacci A, Huguenard JR, Prince DA. Long-lasting self-inhibition of neocortical interneurons mediated by endocannabinoids. Nature. 2004; 431:312–316. [PubMed: 15372034]

Batalla A, Bhattacharyya S, Yucel M, et al. Structural and functional imaging studies in chronic cannabis users: A systematic review of adolescent and adult findings. PLoS ONE. 2013; 8:e55821. [PubMed: 23390554]

Behan B, Connolly C, Datwani S, et al. Response inhibition and elevated parietal-cerebellar correlations in chronic adolescent cannabis users. Neuropharmacology. 2013 EPub ahead of print. 10.1016/j.neuropharm.2013.05.027

Bodor AL, Katona I, Nyiri G, et al. Endocannabinoid signaling in rat somatosensory cortex: Laminar differences and involvement of specific interneuron types. J Neurosci. 2005; 25:6845–6856. [PubMed: 16033894]

Bolla K, Eldreth D, Matochik J, et al. Neural substrates of faulty decision-making in abstinent marijuana users. Neuroimage. 2005; 26:480–492. [PubMed: 15907305]

Broyd SJ, Demanuele C, Debener S, et al. Default-mode brain dysfunction in mental disorders: A systematic review. Neurosci Biobehav Rev. 2009; 33:279–296. [PubMed: 18824195]

Buckner R, Carroll D. Self-Projection and the Brain. Trends Cogn Sci. 2007; 11:49–57. [PubMed: 17188554]

Cavanna A, Trimble M. The Precuneus: A Review of Its Functional Anatomy and Behavioural Correlates. Brain. 2006; 129:564–583. [PubMed: 16399806]

Chang L, Yakupov R, Cloak C, et al. Marijuana use is associated with a reorganized visual-attention network and cerebellar hypoactivation. Brain. 2006; 129:1096–1112. [PubMed: 16585053]

Chanraud S, Pitel AL, Pfefferbaum A, Sullivan EV. Disruption of Functional Connectivity of the Default-Mode Network in Alcoholism. Cereb Cortex. 2011; 21:2272–2281. [PubMed: 21368086]

Chapman L, Chapman J, Raulin M. Body-image aberration in schizophrenia. J Abnorm Psychol. 1978; 87:399–407. [PubMed: 681612]

Collin G, Hulshoff Pol HE, Haijma SV, et al. Impaired cerebellar functional connectivity in schizophrenia patients and their healthy siblings. Front Psychiatry. 2011; 2:73. [PubMed: 22203807]

Cousijn J, Wiers RW, Ridderinkhof KR, et al. Grey matter alterations associated with cannabis use: Results of a VBM study in heavy cannabis users and healthy controls. Neuroimage. 2012; 59:3845–3851. [PubMed: 21982932]

Cox DD, Savoy RL. Functional magnetic resonance imaging (fMRI) “brain reading”: Detecting and classifying distributed patterns of fMRI activity in human visual cortex. Neuroimage. 2003; 19:261–270. [PubMed: 12814577]

Damoiseaux J. Resting-state fMRI as a biomarker for Alzheimer’s disease? Alzheimers Res Ther. 2012; 4:8. [PubMed: 22423634]

Devane WA, Dysarz FA 3rd, Johnson MR, et al. Determination and characterization of a cannabinoid receptor in rat brain. Mol Pharmacol. 1988; 34:605–613. [PubMed: 2848184]

De Wit H. Impulsivity as a Determinant and Consequence of Drug Use: A Review of Underlying Processes. Addict Biol. 2009; 14:22–31. [PubMed: 18855805]

Dumont G, Van Hasselt J, De Kam M, Van Gerven J, Touw D, Buitelaar J, et al. Acute Psychomotor, Memory and Subjective Effects of Mdma and Thc Co-Administration over Time in Healthy Volunteers. J Psychopharmacol. 2011; 25:478–489. [PubMed: 20817749]

Egertova M, Elphick MR. Localisation of cannabinoid receptors in the rat brain using antibodies to the intracellular c-terminal tail of Cb. J Comp Neurol. 2000; 422:159–171. [PubMed: 10842224]

Eggan SM, Lewis DA. Immunocytochemical distribution of the cannabinoid Cb1 receptor in the primate neocortex: A regional and laminar analysis. Cereb Cortex. 2007; 17:175–191. [PubMed: 16467563]

Eggan SM, Melchitzky DS, Sesack SR, et al. Relationship of cannabinoid Cb1 receptor and cholecystokinin immunoreactivity in monkey dorsolateral prefrontal cortex. Neuroscience. 2010; 169:1651–1661. [PubMed: 20542094]

Farkas I, Kallo I, Deli L, et al. Retrograde endocannabinoid signaling reduces gabaergic synaptic transmission to gonadotropin-releasing hormone neurons. Endocrinology. 2010; 151:5818–5829. [PubMed: 20926585]

First, MB.; Spitzer, RL.; Miriam, G., et al. Structured Clinical Interview for DSM-IV-Tr Axis I Disorders, Research Version, Patient Edition with Psychotic Screen (Scid-I/P W/Psy Screen). New York: Biometrics Research, New York State Psychiatric Institute; 2002.

Foldy C, Neu A, Jones MV, et al. Presynaptic, activity-dependent modulation of cannabinoid type 1 receptor-mediated inhibition of GABA release. J Neurosci. 2006; 26:1465–1469. [PubMed: 16452670]

Fridberg DJ, Vollmer JM, O’Donnell BF, et al. Cannabis Users Differ from Non-Users on Measures of Personality and Schizotypy. Psychiatry Res. 2011; 186:46–52. [PubMed: 20813412]

Gaoni Y, Mechoulam R. The isolation and structure of delta-1-tetrahydrocannabinol and other neutral cannabinoids from hashish. J Am Chem Soc. 1971; 93:217–224. [PubMed: 5538858]

Glass M, Dragunow M, Faull RL. Cannabinoid receptors in the human brain: A detailed anatomical and quantitative autoradiographic study in the fetal, neonatal and adult human brain. Neuroscience. 1997; 77:299–318. [PubMed: 9472392]

Grober E, Sliwinski M. Development and validation of a model for estimating premorbid verbal intelligence in the elderly. J Clin Exp Neuropsychol. 1991; 13:933–949. [PubMed: 1779032]

Gruber S, Yurgelun-Todd D. Neuroimaging of marijuana smokers during inhibitory processing: A pilot investigation. Brain Res Cogn Brain Res. 2005; 23:107–118. [PubMed: 15795138]

Haider B, Duque A, Hasenstaub AR, et al. Neocortical network activity in vivo is generated through a dynamic balance of excitation and inhibition. J Neurosci. 2006; 26:4535–4545. [PubMed: 16641233]

Harding I, Solowij N, Harrison B, et al. Functional connectivity in brain networks underlying cognitive control in chronic cannabis users. Neuropsychopharmacology. 2012; 37:1923–1933. [PubMed: 22534625]

Herkenham M, Lynn AB, Little MD, et al. Cannabinoid receptor localization in brain. Proc Natl Acad Sci U S A. 1990; 87:1932–1936. [PubMed: 2308954]

Hester R, Nestor L, Garavan H. Impaired error awareness and anterior cingulate cortex hypoactivity in chronic cannabis users. Neuropsychopharmacology. 2009; 34:2450–2458. [PubMed: 19553917]

Hill EL, Gallopin T, Ferezou I, et al. Functional Cb1 receptors are broadly expressed in neocortical gabaergic and glutamatergic neurons. J Neurophysiol. 2007; 97:2580–2589. [PubMed: 17267760]

Hirvonen J, Goodwin RS, Li CT, et al. Reversible and Regionally Selective Downregulation of Brain Cannabinoid Cb(1) Receptors in Chronic Daily Cannabis Smokers. Mol Psychiatry. 2012; 17:642–649. [PubMed: 21747398]

Houck J, Bryan A, Feldstein Ewing S. Functional connectivity and cannabis use in high-risk adolescents. Am J Drug Alcohol Abuse. 2013; 39:414–423. [PubMed: 24200211]

Jager G, Van Hell H, De Win M, et al. Effects of frequent cannabis use on hippocampal activity during an associative memory task. Eur Neuropsychopharmacol. 2007; 17:289–297. [PubMed: 17137758]

Johnson B, Zhang K, Gay M, et al. Alteration of brain default network in subacute phase of injury in concussed individuals: Resting-state fMRI study. Neuroimage. 2012; 59:511–518. [PubMed: 21846504]

Katona I, Sperlagh B, Magloczky Z, et al. Gabaergic interneurons are the targets of cannabinoid actions in the human hippocampus. Neuroscience. 2000; 100:797–804. [PubMed: 11036213]

Kim D, Skosnik P, Cheng H, et al. Structural network topology revealed by white matter tractography in cannabis users: A graph theoretical analysis. Brain Connect. 2011; 1:473–483. [PubMed: 22432904]

King G, Ernst T, Deng W, et al. Altered brain activation during visuomotor integration in chronic active cannabis users: Relationship to cortisol levels. J Neurosci. 2011; 311:17923–17931. [PubMed: 22159107]

Kriegeskorte N, Goebel R, Bandettini P. Information-based functional brain mapping. Proc Natl Acad Sci U S A. 2006; 103:3863–3868. [PubMed: 16537458]

Lohmann G, Volz K, Ullsperger M. Using non-negative matrix factorization for single-trial analysis of fMRI data. Neuroimage. 2007; 37:1148–1160. [PubMed: 17662621]

Matochik J, Eldreth D, Cadet J, et al. Altered brain tissue composition in heavy marijuana users. Drug Alcohol Depend. 2005; 77:23–30. [PubMed: 15607838]

Meier TB, Desphande AS, Vergun S, et al. Support vector machine classification and characterization of age-related reorganization of functional brain networks. Neuroimage. 2012; 60:601–613. [PubMed: 22227886]

Newlin DB, Renton RM. A Self in the Mirror: Mirror Neurons, Self-Referential Processing, and Substance Use Disorders. Subst Use Misuse. 2010; 45:1697–1726. [PubMed: 20590396]

O'Carroll R, Walker M, Dunan J, et al. Selecting controls for schizophrenia research studies: The use of the National Adult Reading Test (Nart) is a measure of premorbid ability. Schizophr Res. 1992; 8:137–141. [PubMed: 1457392]

Orr C, Morioka R, Behan B, et al. Altered resting-state connectivity in adolescent cannabis users. Am J Drug Alcohol Abuse. 2013; 39:372–381. [PubMed: 24200207]

Patton J, Stanford M, Barratt E. Factor structure of the Barratt Impulsiveness Scale. J Clin Psychol. 1995; 51:768–774. [PubMed: 8778124]

Pertwee RG. Pharmacology of cannabinoid Cb1 and Cb2 receptors. Pharmacol Ther. 1997; 74:129–180. [PubMed: 9336020]

Pertwee RG. Pharmacology of cannabinoid receptor ligands. Curr Med Chem. 1999; 6:635–664. [PubMed: 10469884]

Pertwee RG, Howlett AC, Abood ME, et al. International Union of Basic and Clinical Pharmacology. LXXIX. Cannabinoid receptors and their ligands: beyond CB_1 and CB_2. Pharmacol Rev. 2010; 62:588–631. [PubMed: 21079038]

Pujol J, Blanco-Hinojo L, Batalla A, et al. Functional Connectivity Alterations in Brain Networks Relevant to Self-Awareness in Chronic Cannabis Users. J Psychiatr Res. 2014; 51:68–78. [PubMed: 24411594]

Raine A. The SPQ: A scale for the assessment of schizotypal personality based on DSM-III-R criteria. Schizophr Bull. 1991; 17:555–564. [PubMed: 1805349]

Ranganathan M, D'Souza DC. The acute effects of cannabinoids on memory in humans: A review. Psychopharmacology (Berl). 2006; 188:425–444. [PubMed: 17019571]

Roberts GM, Garavan H. Evidence of Increased Activation Underlying Cognitive Control in Ecstasy and Cannabis Users. Neuroimage. 2010; 52:429–435. [PubMed: 20417713]

Schweinsburg A, Nagel B, Schweinsburg B, et al. Abstinent adolescent marijuana users show altered fMRI response during spatial working memory. Psychiatry Res. 2008; 163:40–51. [PubMed: 18356027]

Schweinsburg A, Schweinsburg B, Medina K, et al. The influence of recency of use on fMRI response during spatial working memory in adolescent marijuana users. J Psychoactive Drugs. 2010; 42:401–412. [PubMed: 21053763]

Sewell RA, Skosnik PD, Garcia-Sosa I, et al. (Behavioral, cognitive and psychophysiological effects of cannabinoids: Relevance to psychosis and schizophrenia). Rev Bras Psiquiatr. 2010; 32(Suppl 1):S15–30. [PubMed: 20512267]

Sim-Selley LJ, Schechter NS, Rorrer WK, et al. Prolonged recovery rate of Cb1 receptor adaptation after cessation of long-term cannabinoid administration. Mol Pharmacol. 2006; 70:986–996. [PubMed: 16760363]

Skosnik PD, D'Souza DC, Steinmetz AB, et al. The effect of chronic cannabinoids on broadband EEG neural oscillations in humans. Neuropsychopharmacology. 2012; 37:2184–2193. [PubMed: 22713908]

Skosnik PD, Edwards CR, O'Donnell BF, et al. Cannabis use disrupts eyeblink conditioning: Evidence for cannabinoid modulation of cerebellar-dependent learning. Neuropsychopharmacology. 2008; 33:1432–1440. [PubMed: 17637608]

Skosnik PD, Krishnan GP, Aydt EE, et al. Psychophysiological evidence of altered neural synchronization in cannabis use: Relationship to schizotypy. Am J Psychiatry. 2006; 163:1798–1805. [PubMed: 17012692]

Smith SM, Fox PT, Miller KL, et al. Correspondence of the brain's functional architecture during activation and rest. Proc Natl Acad Sci U S A. 2009; 106:13040–13045. [PubMed: 19620724]

Stanford M, Mathias C, Dougherty D, et al. Fifty years of the Barratt Impulsiveness Scale: An update and review. Pers Indiv Dif. 2009; 47:385–395.

Tsou K, Brown S, Sanudo-Pena MC, et al. Immunohistochemical distribution of cannabinoid Cb1 receptors in the rat central nervous system. Neuroscience. 1998; 83:393–411. [PubMed: 9460749]

Van Dijk K, Sabuncu M, Buckner R. The influence of head motion on intrinsic functional connectivity MRI. NeuroImage. 2012; 59:431–438. [PubMed: 21810475]

Van Hell H, Vink M, Ossewaarde L, et al. Chronic effects of cannabis use on the human reward system: An fMRI study. Eur Neuropsychopharmacol. 2009; 20:153–163. [PubMed: 20061126]

Villares J. Chronic use of marijuana decreases cannabinoid receptor binding and mRNA expression in the human brain. Neuroscience. 2007; 145:323–334. [PubMed: 17222515]

Wang W, Wang YR, Qin W, et al. Changes in Functional Connectivity of Ventral Anterior Cingulate Cortex in Heroin Abusers. Chin Med J (Engl). 2010; 123:1582–1588. [PubMed: 20819516]

Weinstein A, Brickner O, Lerman H, et al. A Study Investigating the Acute Dose-Response Effects of 13 Mg and 17 Mg Delta 9- Tetrahydrocannabinol on Cognitive-Motor Skills, Subjective and Autonomic Measures in Regular Users of Marijuana. J Psychopharmacol. 2008; 22:441–451. [PubMed: 18635724]

Wesley M, Hanlon C, Porrino L. Poor decision-making by chronic marijuana users is associated with decreased functional responsiveness to negative consequences. Psychiatry Res. 2011; 191:51–59. [PubMed: 21145211]

Yücel M, Solowij N, Respondek C, et al. Regional brain abnormalities associated with long-term heavy cannabis use. Arch Gen Psychiatry Res. 2008; 65:694–701.

Zhang Y, Tian J, Yuan K, et al. Distinct resting-state brain activities in heroin-dependent individuals. Brain Res. 2011; 1402:46–53. [PubMed: 21669407]

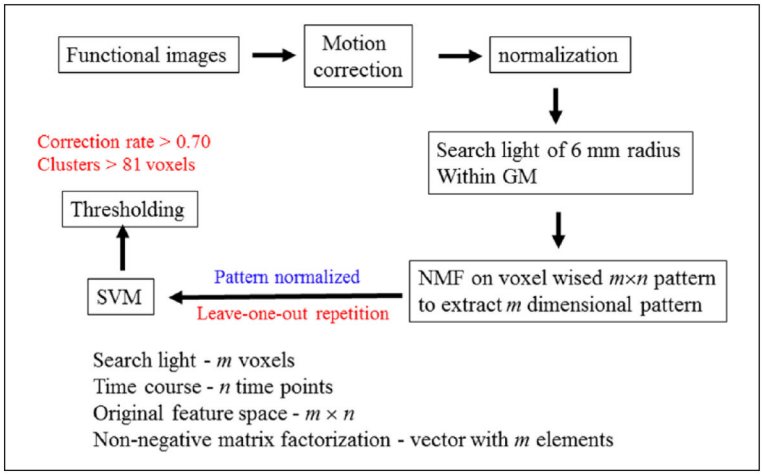

Figure 1.

Schematic drawing the data processing pipeline for local multi-voxel pattern analysis (MVPA) analysis. NMF: non-negative matrix factorization; SVM: support vector machine; GM: gray matter.

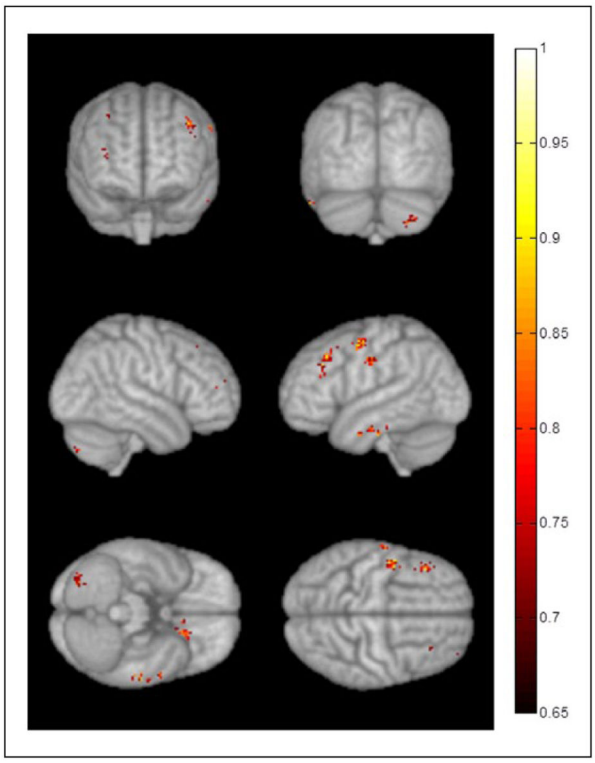

Figure 2.
Results of local multi-voxel pattern analysis (MVPA) analysis of resting state functional magnetic resonance imaging (fMRI) data displayed on 3D rendered brain showing distinct clusters between cannabis users and normal controls.

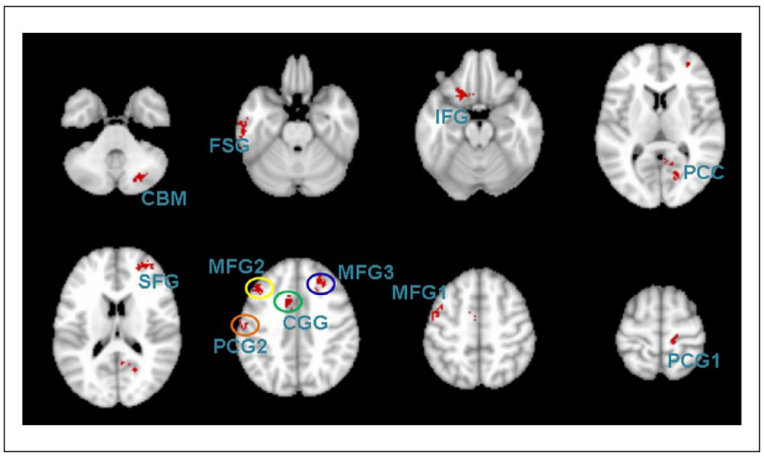

Figure 3.

Results of local multi-voxel pattern analysis (MVPA) analysis of resting state functional magnetic resonance imaging (fMRI) data displayed on 2D slices showing 11 clusters with corresponding brain regions. CBM: cerebellum; CGG: cingulate gyrus; FSG: fusiform gyrus; IFG: inferior frontal gyrus; MFG: middle frontal gyrus; PCC: posterior cingulate cortex; PCG: precentral gyrus; SFG: superior frontal gyrus.

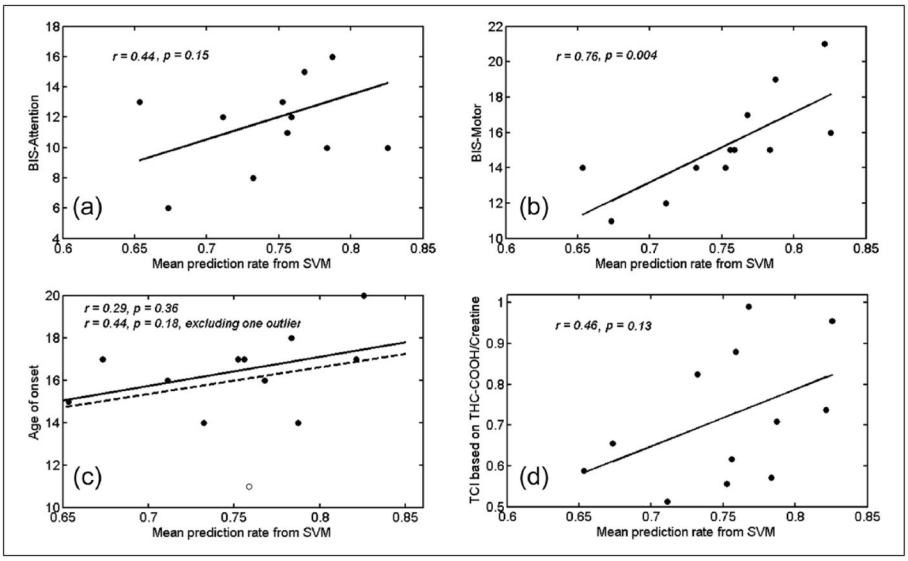

Figure 4.

Scatter plots between some behavior measurements and mean accuracy rate from support vector machine (SVM) of all the voxels in the map of Figure 2 for cannabis users. Only behavior measurements with significant difference between the two groups were selected, including (a) Barratt Impulsiveness Scale (BIS)-Attention, (b) BIS-Motor, and (c) age of onset of cannabis use; (d) is tetrahydrocannabinol (THC) classification index (TCI) based on THC-COOH/creatine ratio.

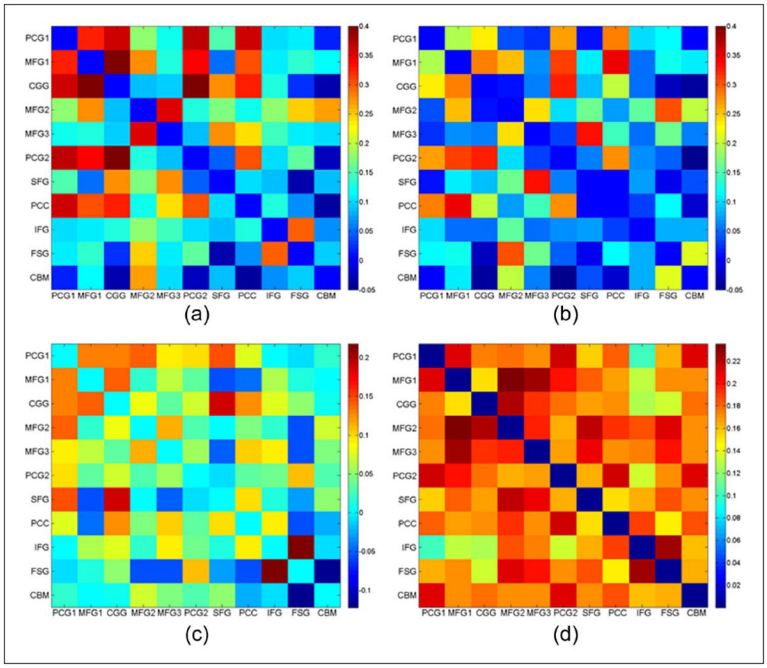

Figure 5.

Mean functional connectivity between the eleven distinct regions is represented by an adjacent matrix for (a) cannabis users (CB group) and (b) controls (CTL group). The diagonal elements were set to zero to exclude self-connectivity. Higher overall connectivity strength was observed for the CB group, as indicated by their difference (c). The corresponding standard deviation of connectivity between each pair of distinct regions across all subjects is shown in (d). CBM: cerebellum; CGG: cingulate gyrus; FSG: fusiform gyrus; IFG: inferior frontal gyrus; MFG: middle frontal gyrus; PCC: posterior cingulate cortex; PCG: precentral gyrus; SFG: superior frontal gyrus.

Table 1

Demographic, substance use, and characteristics of study participants.

	Group, mean±SD		*p* value
Characteristics	**Cannabis users (*n*=12)**	**Controls (*n*=13)**	
Age (years)	19.33±0.98	21.62±3.84	0.06
Education (years)	12.75±0.75	13.92±1.88	0.09
Sex (% male)	12 (100%)	13 (100%)	
Handedness (% right)	11 (93%)	13 (100%)	
Drinks/week (g)	78.17±74.43	23.69±65.26	0.06
Cigarettes in past week	1.54±2.66	0	<0.05
PAS	2.08±1.98	0.62±1.19	<0.03
Total SPQ score	12.58±9.92	5.46±5.77	<0.04
ANART score	13.58±9.92	14.58±4.96	0.59
BIS: Attention	12.08±3.53	9.38±2.10	<0.03
BIS: Motor	15.25±2.77	12.62±2.40	<0.02
Age of first use (years)	16.00±2.26	N/A	
Duration (years)	3.33±2.39	N/A	
Use in past week (joints)	12.83±10.93	N/A	
Relative translational head motion (mm)	0.055±0.037	0.046±0.015	0.51
Relative rotational head motion (mm)	0.038±0.016	0.039±0.020	0.91
Absolute translational head motion (mm)	0.19±0.15	0.31±0.32	0.24
Absolute rotational head motion (mm)	0.17±0.13	0.29±0.32	0.25

ANART: American National Adult Reading Test; BIS: Barrett Impulsiveness Scale factor score; N/A: not applicable; PAS: Perceptual Aberration Scale; SD: standard deviation; SPQ: schizotypal personality questionnaire.

Table 2

Name of distinct regions between cannabis users and normal controls from local multi-voxel pattern analysis (MVPA) analysis. The Montreal Neurological Institute (MNI) coordinates and cluster size of the regions are also listed.

Regions	Abbreviation	MNI coordinates	Cluster size	Accuracy
Precentral gyrus	PCG1 (R)	(14, −30, 64)	82	75.5%
Middle frontal gyrus	MFG1 (L)	(−44, 2, 52)	84	76.9%
Cingulate gyrus	CGG	(−8, 6, 48)	118	77.1%
Middle frontal gyrus	MFG2 (L)	(−42, 26, 40)	102	76.7%
Middle frontal gyrus	MFG3 (R)	(26, 34, 40)	91	76.6%
Precentral gyrus	PCG2 (L)	(−60, −12, 38)	83	75.6%
Superior frontal gyrus	SFG (R)	(30, 52, 16)	101	76.3%
Posterior cingulate cortex	PCC (R)	(18, −68, 8)	127	75.4%
Inferior frontal gyrus	IFG (L)	(−18, 20, −20)	100	77.4%
Fusiform gyrus	FSG (L)	(−58, −16, −26)	87	76.0%
Cerebellum	CBM (R)	(28, −74, −38)	115	75.2%

R: right; L: left.

Table 3

In the support vector machine (SVM) analysis, feature space was chosen to be the functional connectivity between clusters. The classifying accuracy of SVM was tested for different thresholds of the connectivity strength. The number of features is also listed.

Threshold	None	0.05	0.1	0.15	0.20	0.25
Number of features	55	47	28	21	15	14
Overall accuracy	84%	84%	88%	88%	88%	88%
Accuracy for CTL	85%	85%	92%	85%	92%	85%
Accuracy for CB	83%	83%	83%	92%	83%	92%

CTL: control group; THC: tetrahydrocannabinol.